

Figure S1. Semivariogram of the temporal variability of pH offset differences for the entire study period. Light grey points in the background represent all possible pairs of pH offset differences, while dark circles indicate the mean values calculated using moving bins.

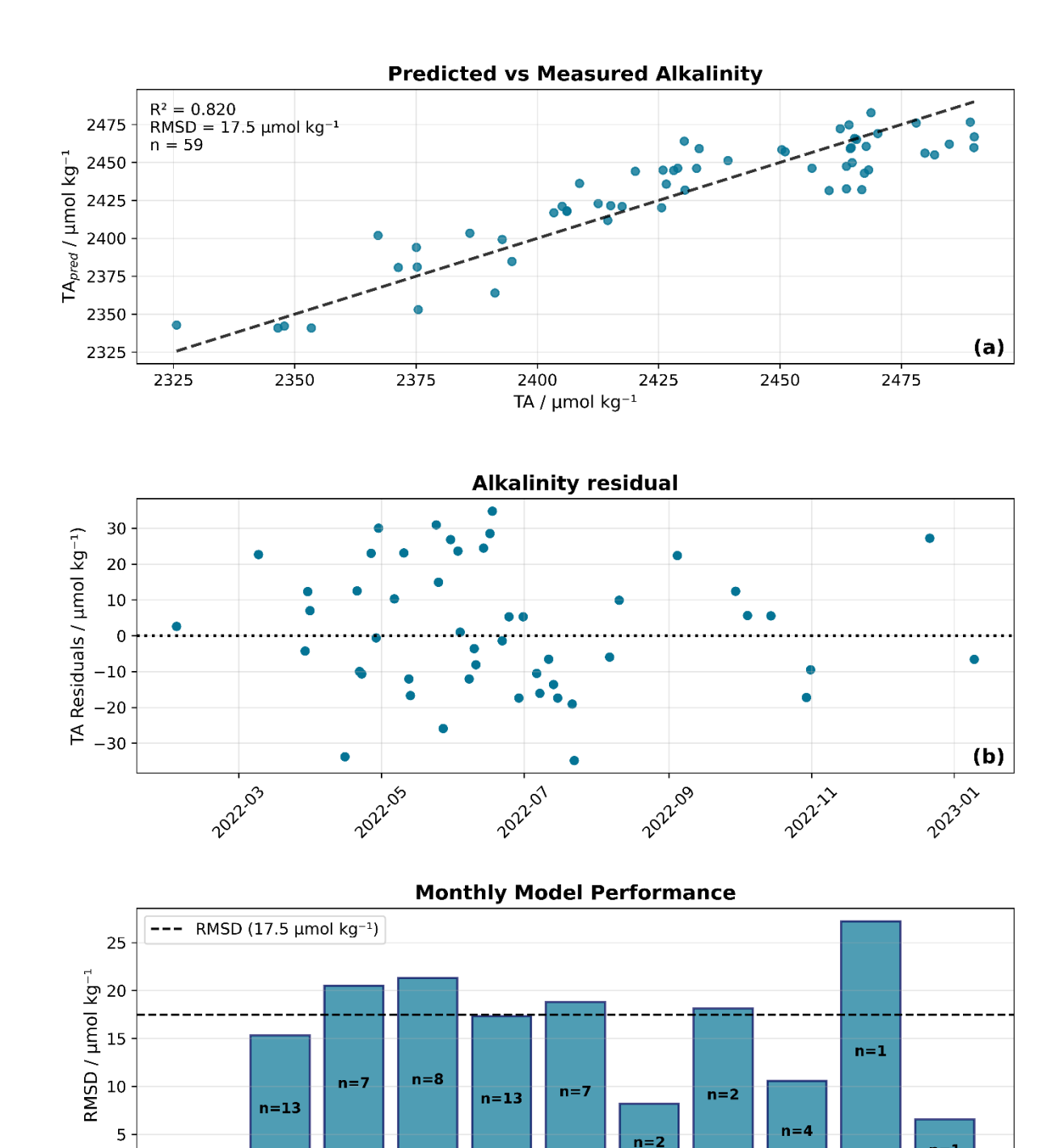


Figure S2. Model performance evaluation for TA predictions. (a) Shows predicted versus measured TA values, with the 1:1 line and statistical metrics, including coefficient of determination (R²), root mean square deviation (RMSD), and sample size (n). **(b)** Time series of TA residuals (measured minus predicted values) showing temporal patterns in model performance, with the zero-line indicating perfect prediction (dotted black line). **(c)** Monthly model performance expressed as RMSD values. The horizontal dashed line indicates the overall RMSD across all months. Sample sizes (n) for each month are displayed within the bars.

Mu

1/1/

hay

MIG

sep

oč

oec

0

4eb

Nat

PQ

(c)

Par

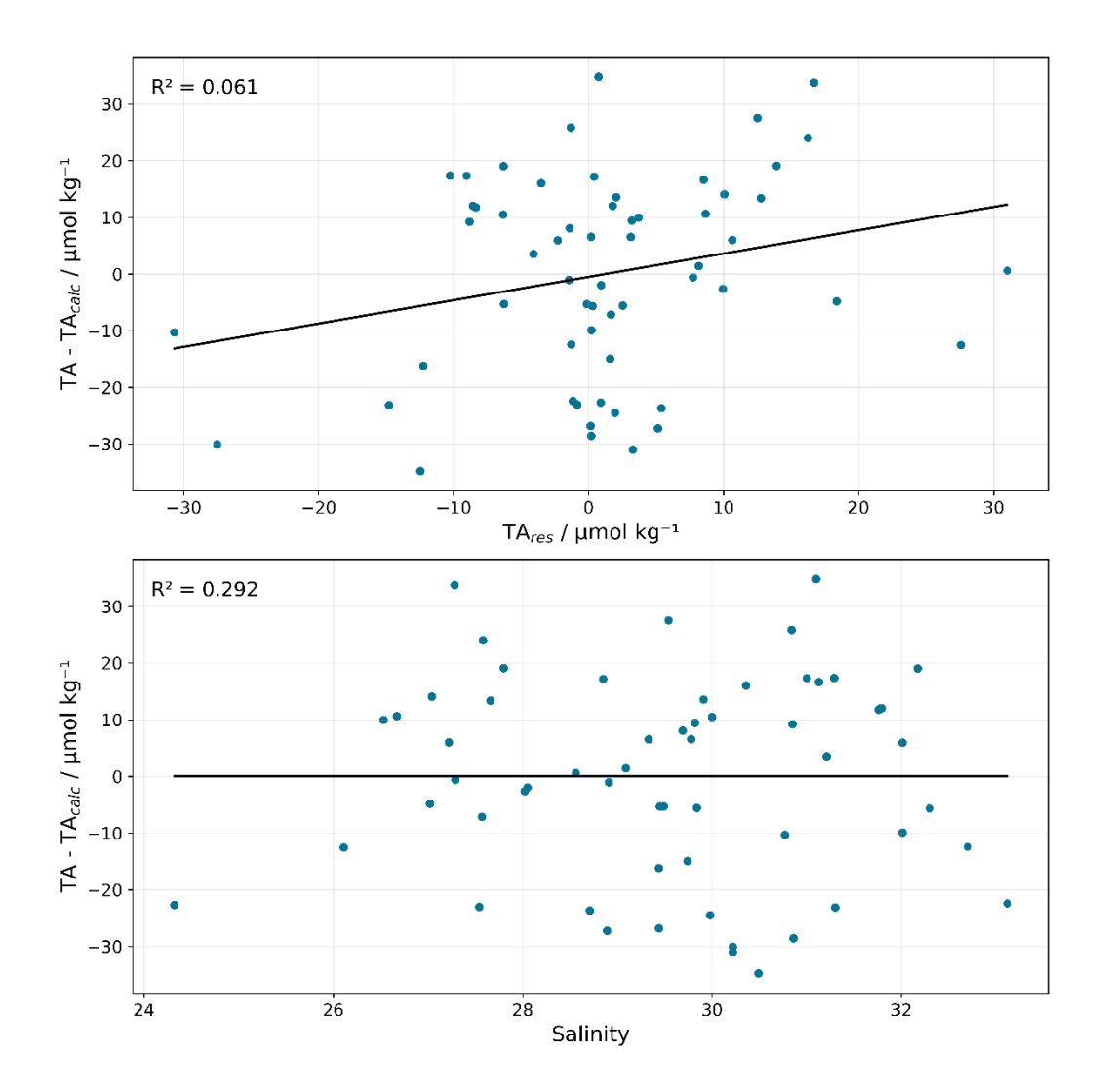


Figure S3. Relationship between TA_{res} and OrgAlk ($TA - TA_{calc}$) and salinity. **(a)** Correlation between $TA - TA_{calc}$ and TA_{res} , with linear regression line (black) and coefficient of determination (R^2). **(b)** Correlation between salinity and TA_{res} , with linear regression line (black) and R^2 .

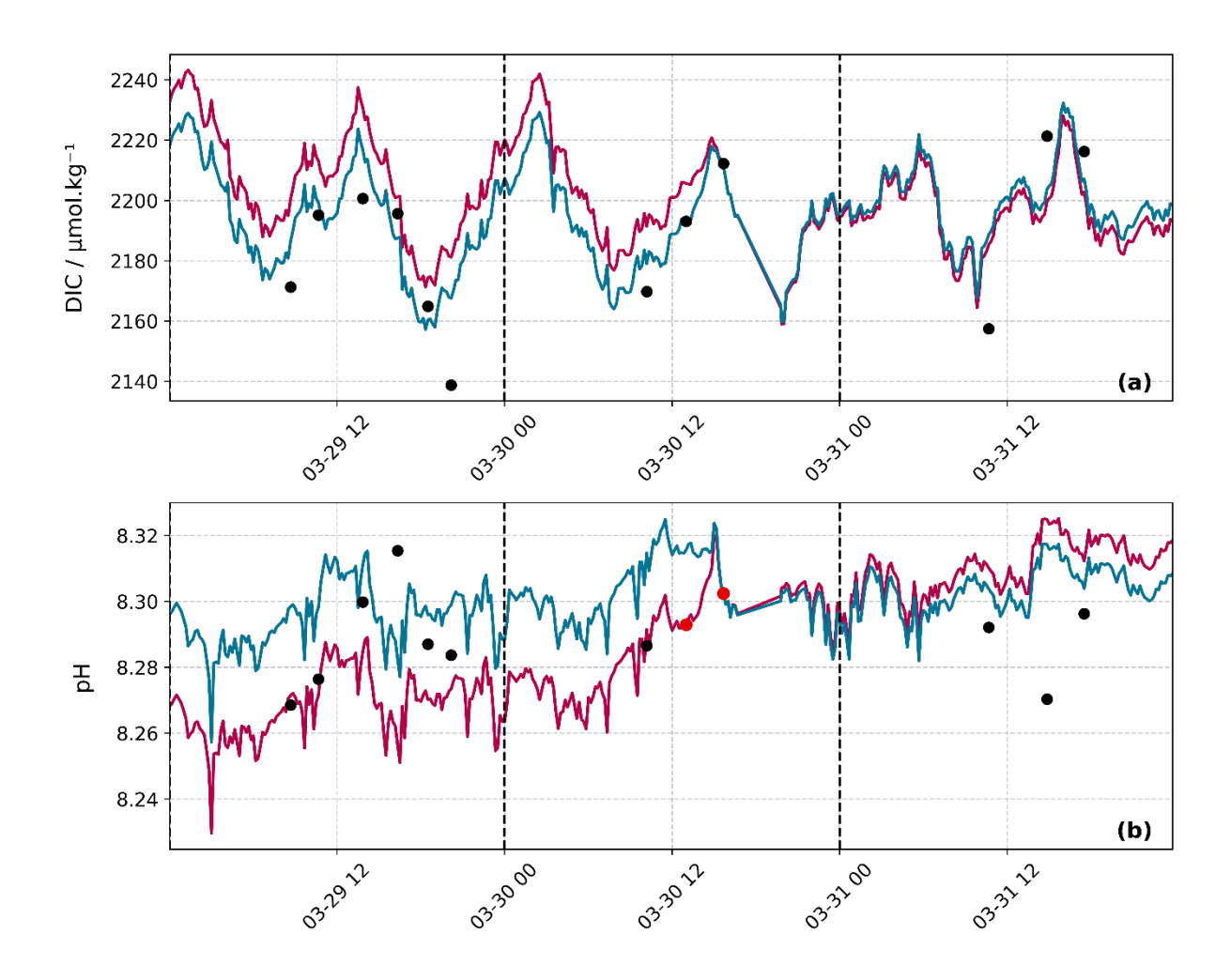


Figure S4: pH calibration approach on high-resolution DIC calculations during a 72-hour period.

In (a): DIC calculated from TA_{pred} and pH sensor data using different calibration strategies: blue line represents the DIC that was calculated suing pH calibrated with all available high-resolution pH samples. Red line represents the DIC calculated using pH recalibrated based on only two reference points indicated in red in (b). Black scatter points indicate all measured DIC.

In (b): Corresponding high-resolution pH time series. Black scatter points indicate all measured pH values. The blue line represents the calibrated pH using the full dataset and in red line the pH that was recalibrated using two selected calibration points shown in red in (b). Vertical dashed lines represent the daily boundaries.

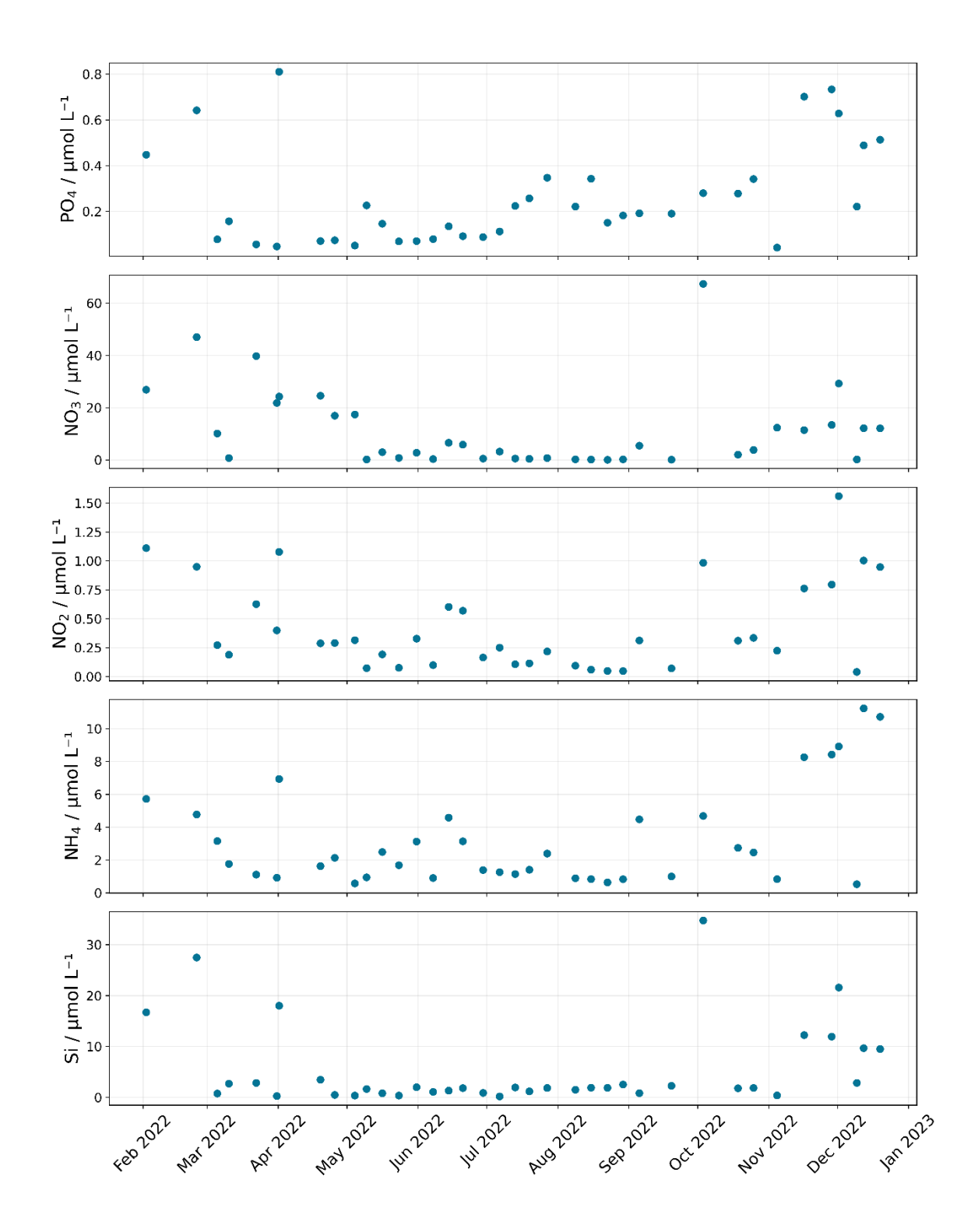


Figure S5. Seasonal variability of nutrient concentrations from February 2022-January 2023. All concentrations are in μ mol L⁻¹. PO_4^{3-} : phosphate, NO_3^- : nitrate, NO_2^- : nitrite, and Si: silicate.

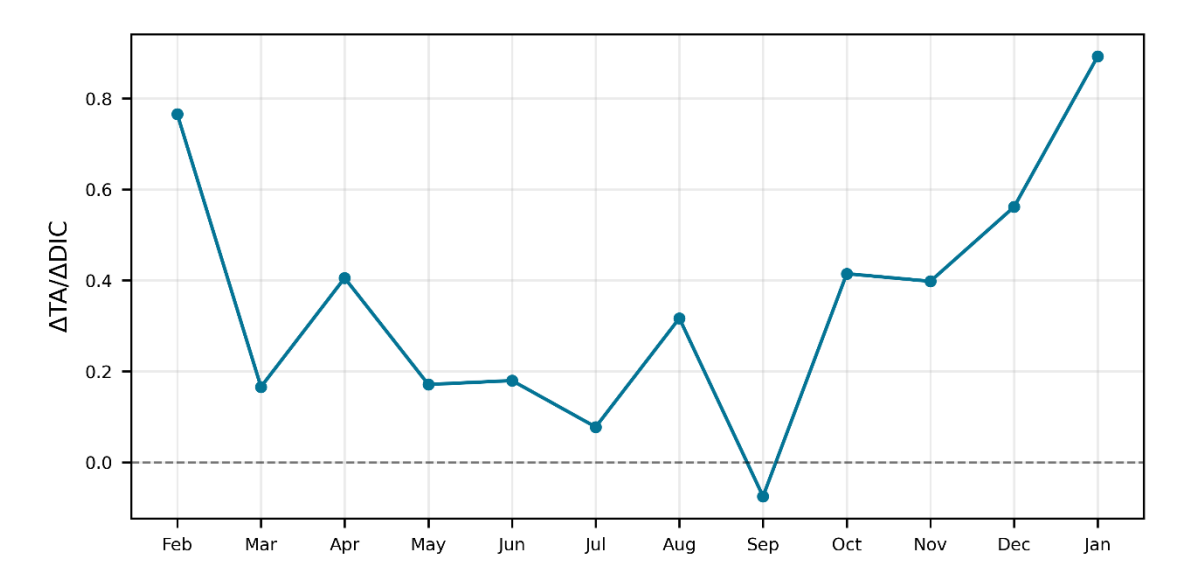


Figure S6. Temporal variability of TA/DIC ratio in the Wadden Sea.

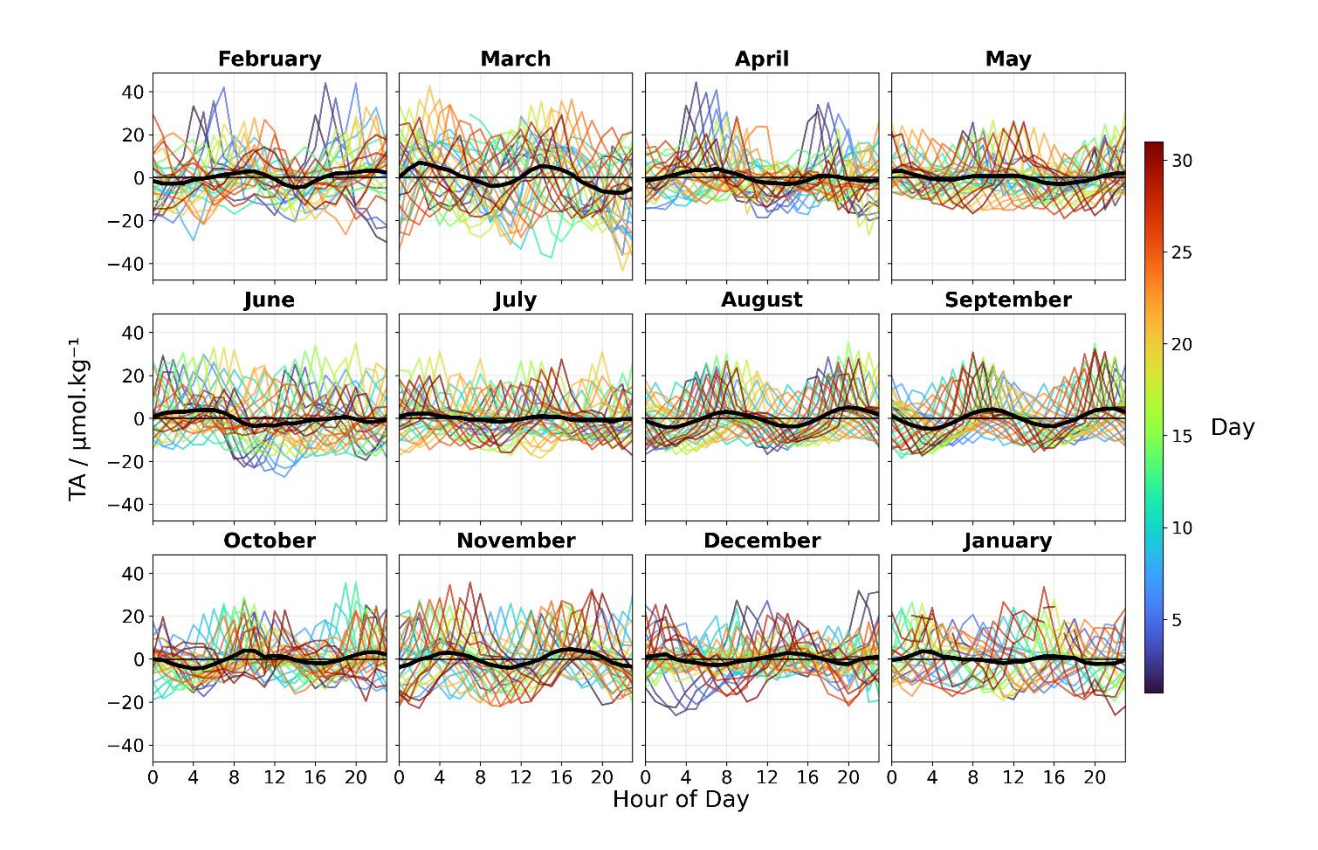


Figure S7. Seasonal diurnal variability of TA anomalies between February 2022-January 2023.

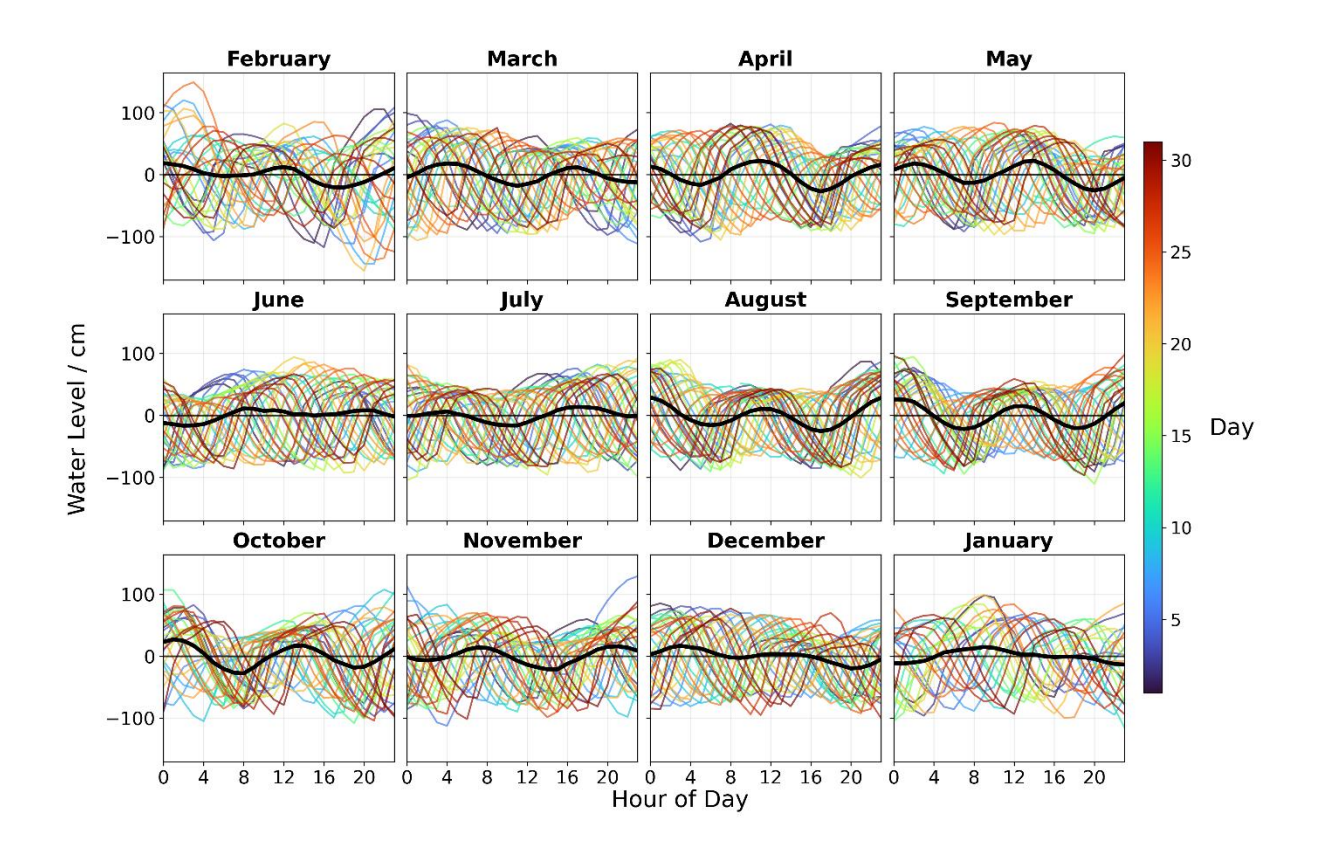


Figure S8. Seasonal diurnal variability of water level anomalies between February 2022-January 2023.

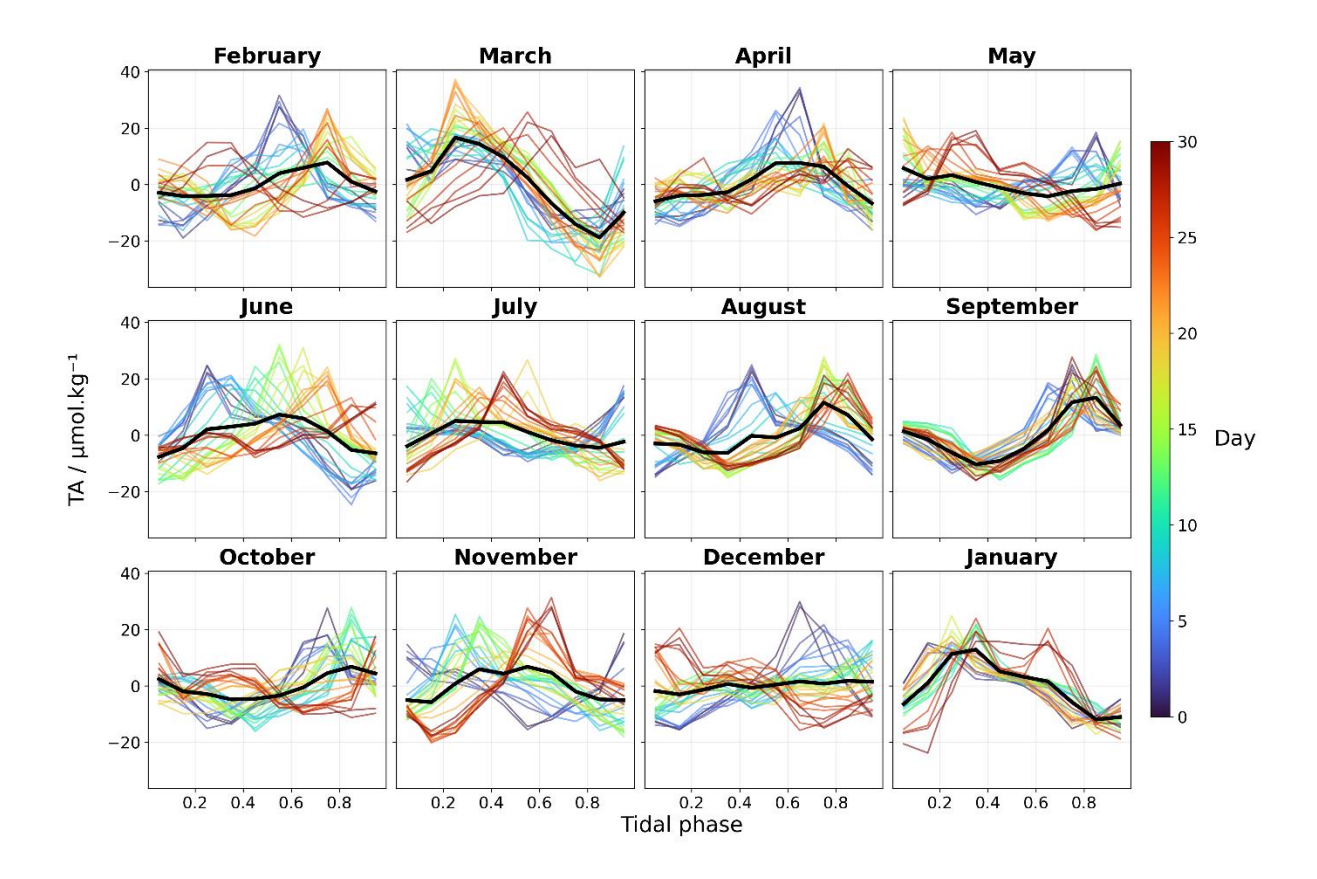


Figure S9. Tidal phase analysis variability of TA anomalies between February 2022-January 2023.

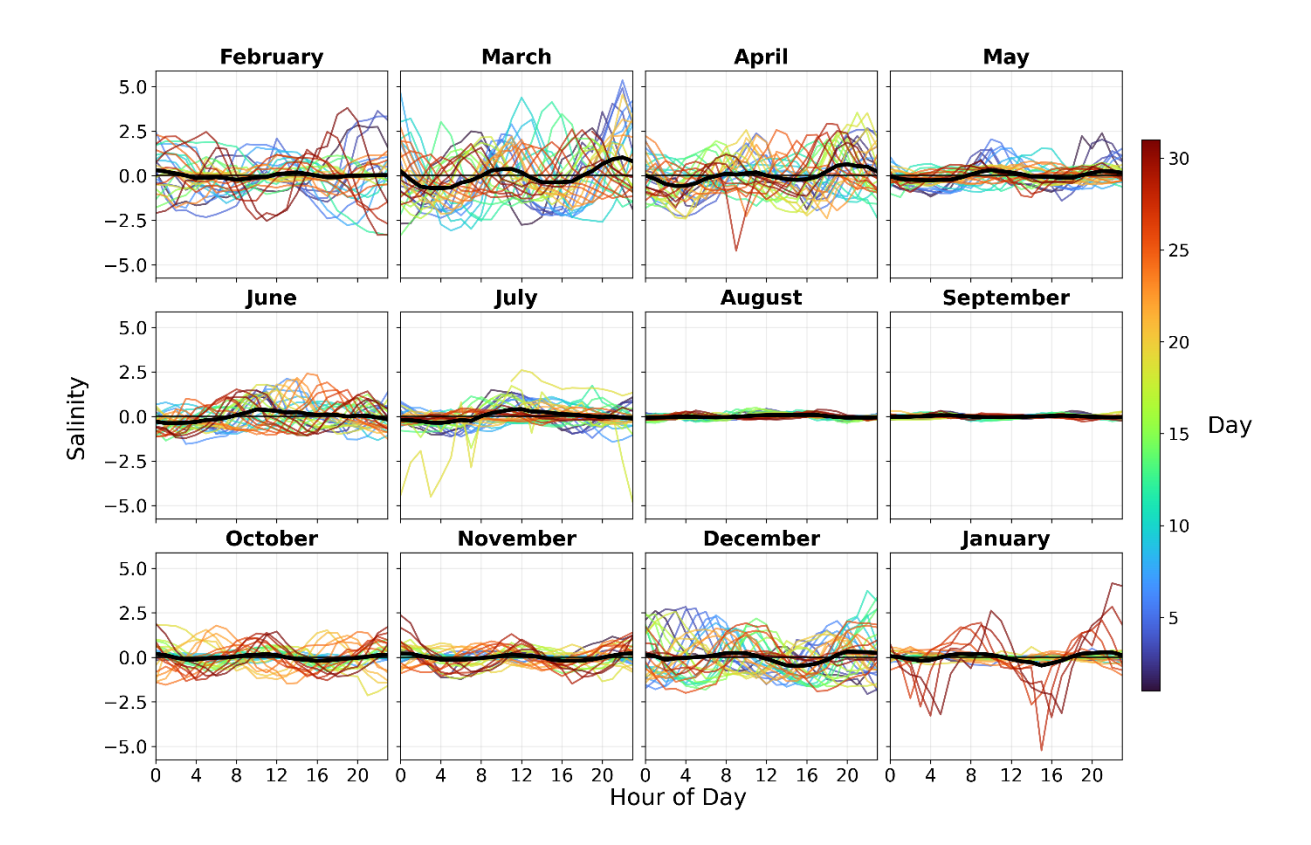


Figure S10. Seasonal diurnal variability of salinity anomalies between February 2022-January 2023.

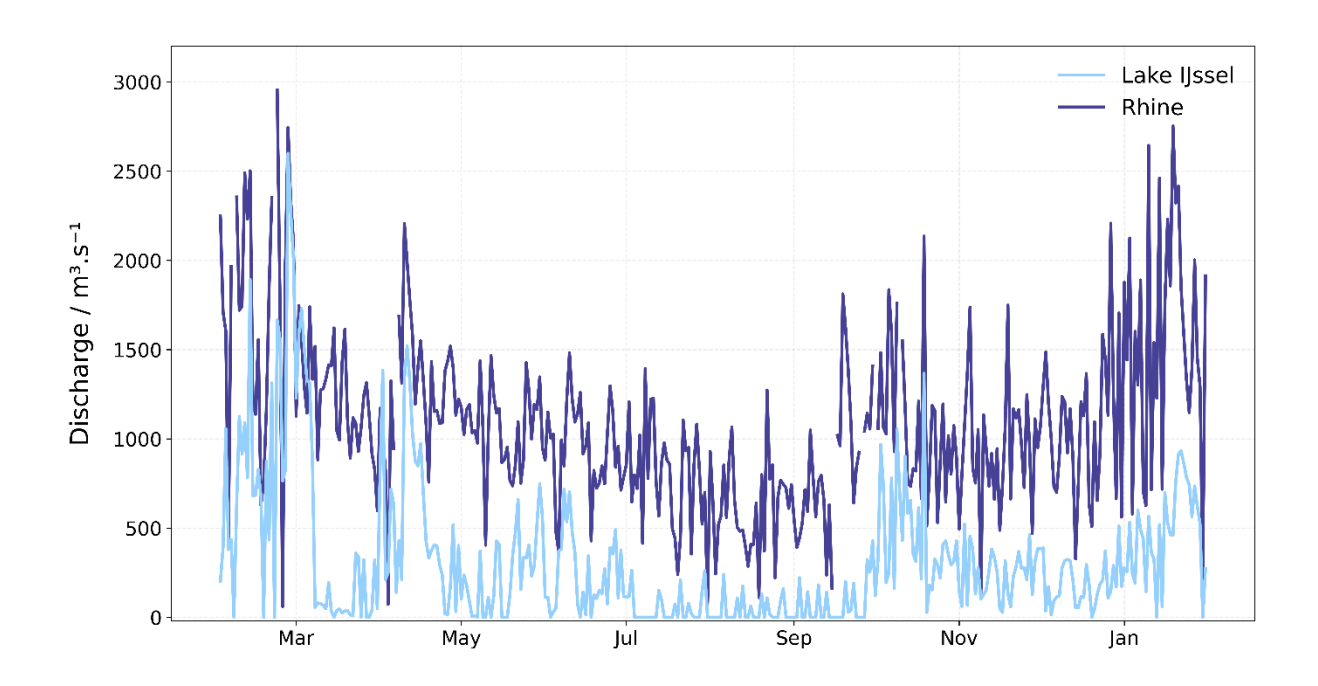


Figure S11. Daily river discharge of the Rhine River (dark blue) and Lake IJssel (light blue) for the period 2022-2023. Discharge values are given in cubic meters per second (m³ s⁻¹).

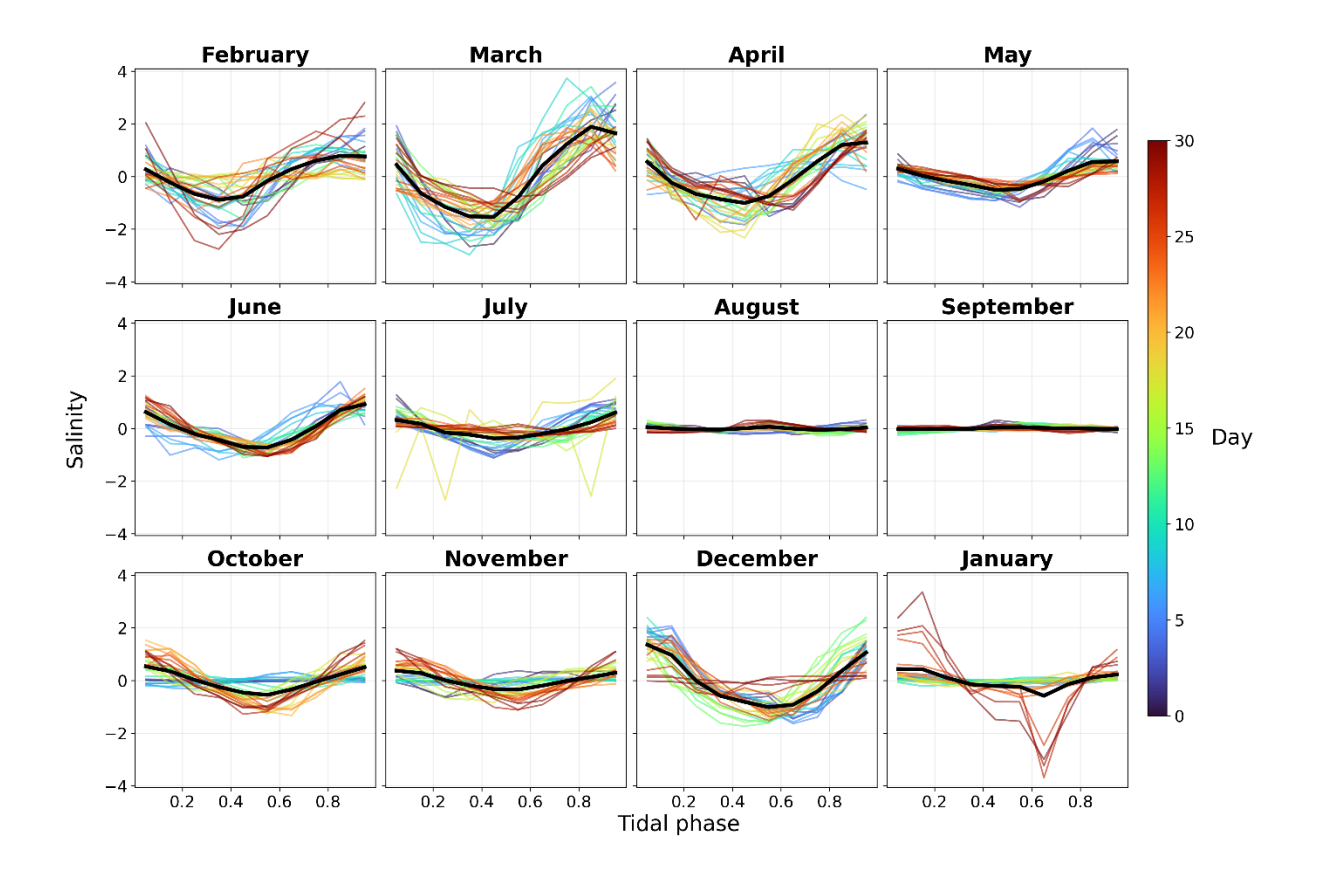


Figure S12. Tidal phase analysis variability of salinity anomalies between February 2022-January 2023.

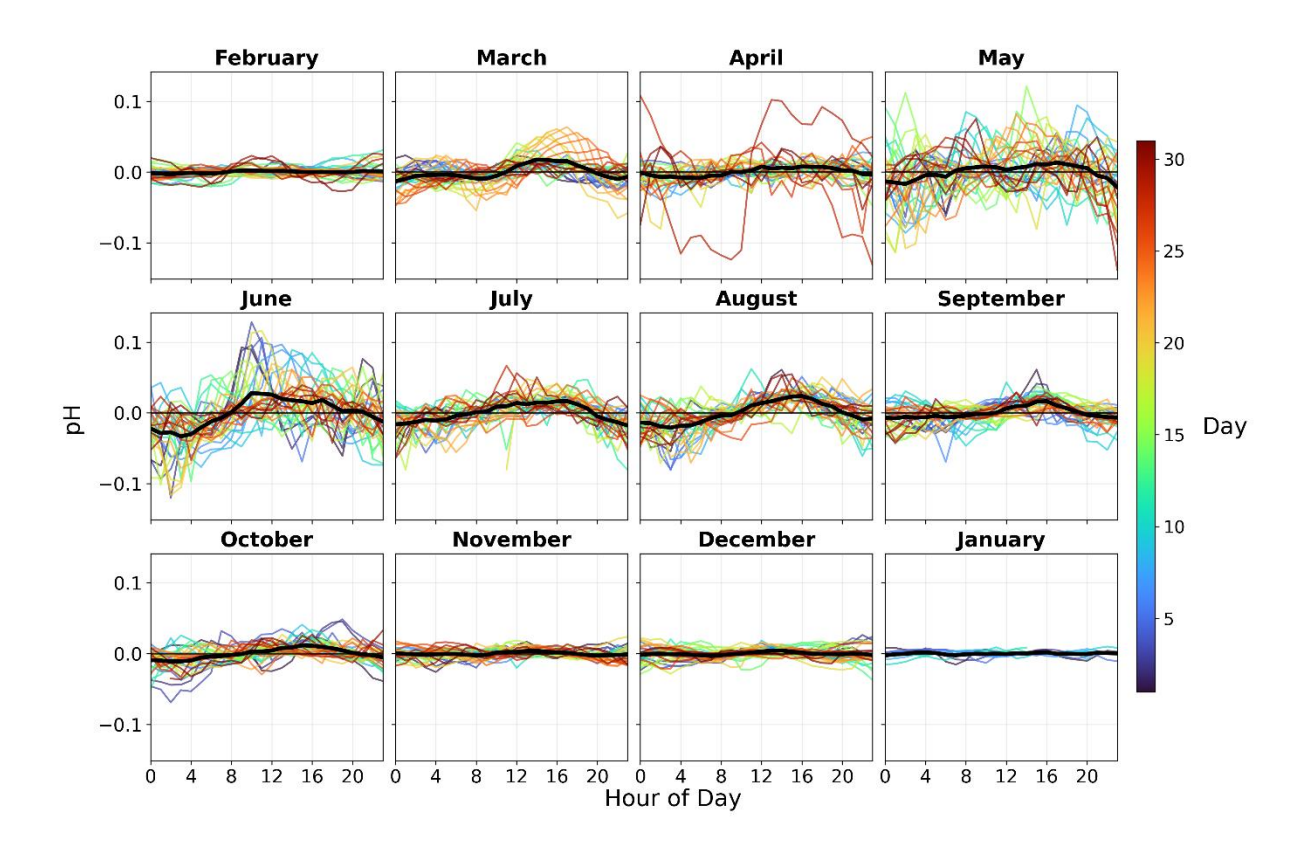


Figure S13. Seasonal diurnal variability of pH anomalies between February 2022-January 2023.

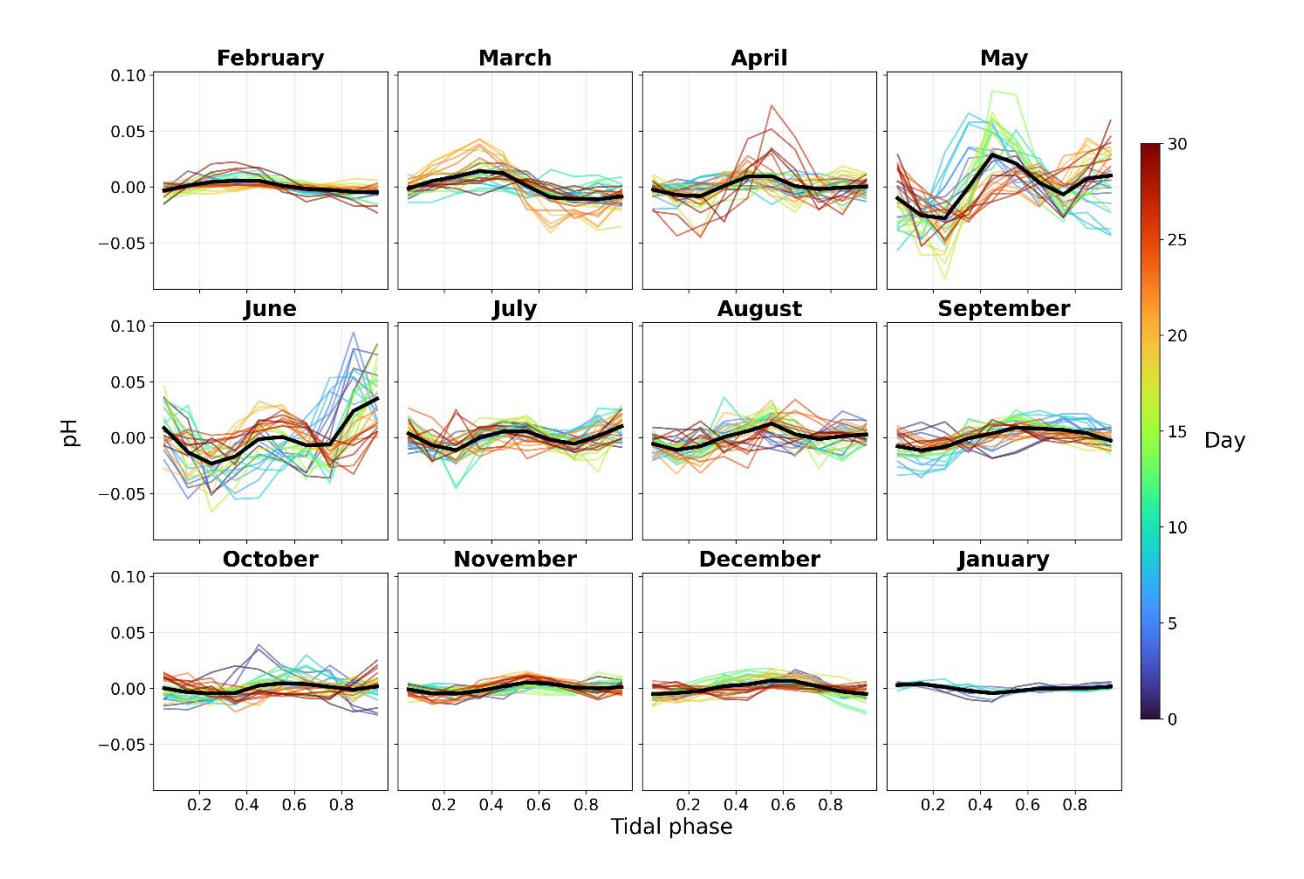


Figure S14. Tidal phase analysis variability of pH anomalies between February 2022-January 2023.

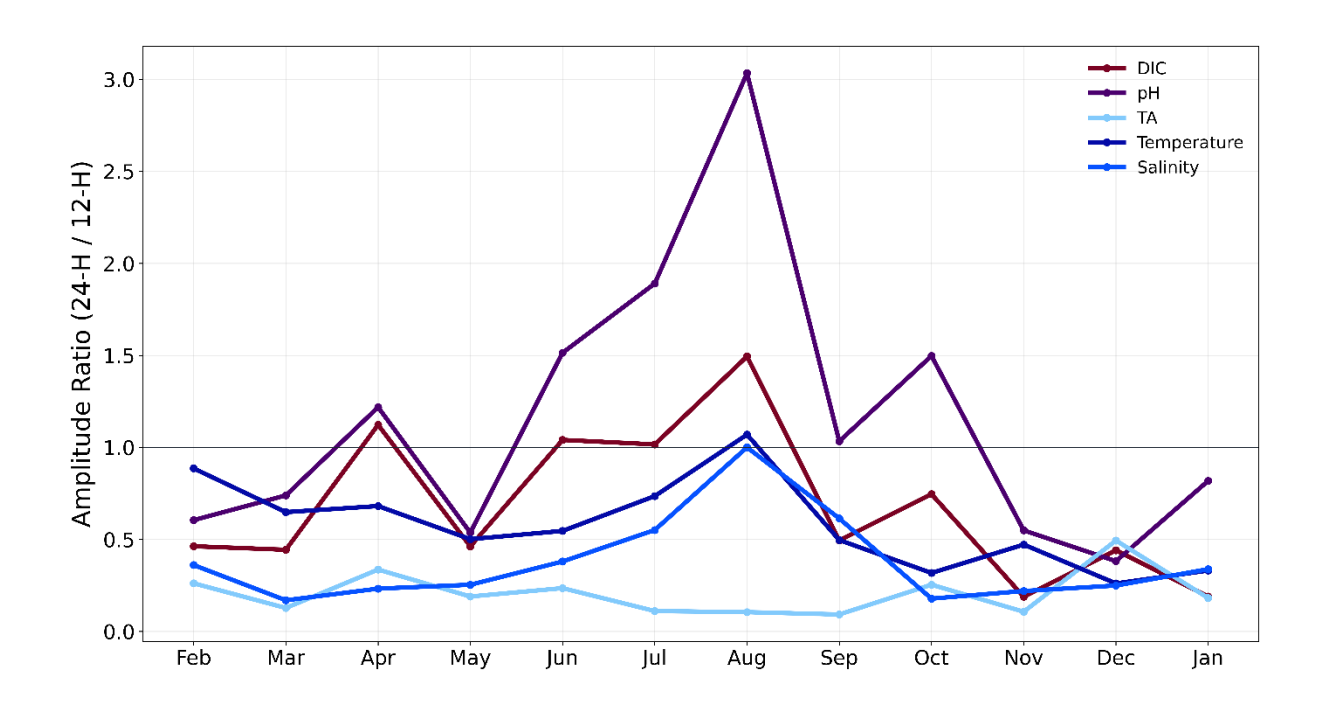


Figure S15. Fourier analysis showing amplitude ratio between the 24-H and 12-H frequencies.

The amplitude ratio is plotted for pH, TA, DIC, temperature and salinity. Values above 1 indicate a stronger diel signal, while values below 1 indicate a stronger semi-diurnal signal.

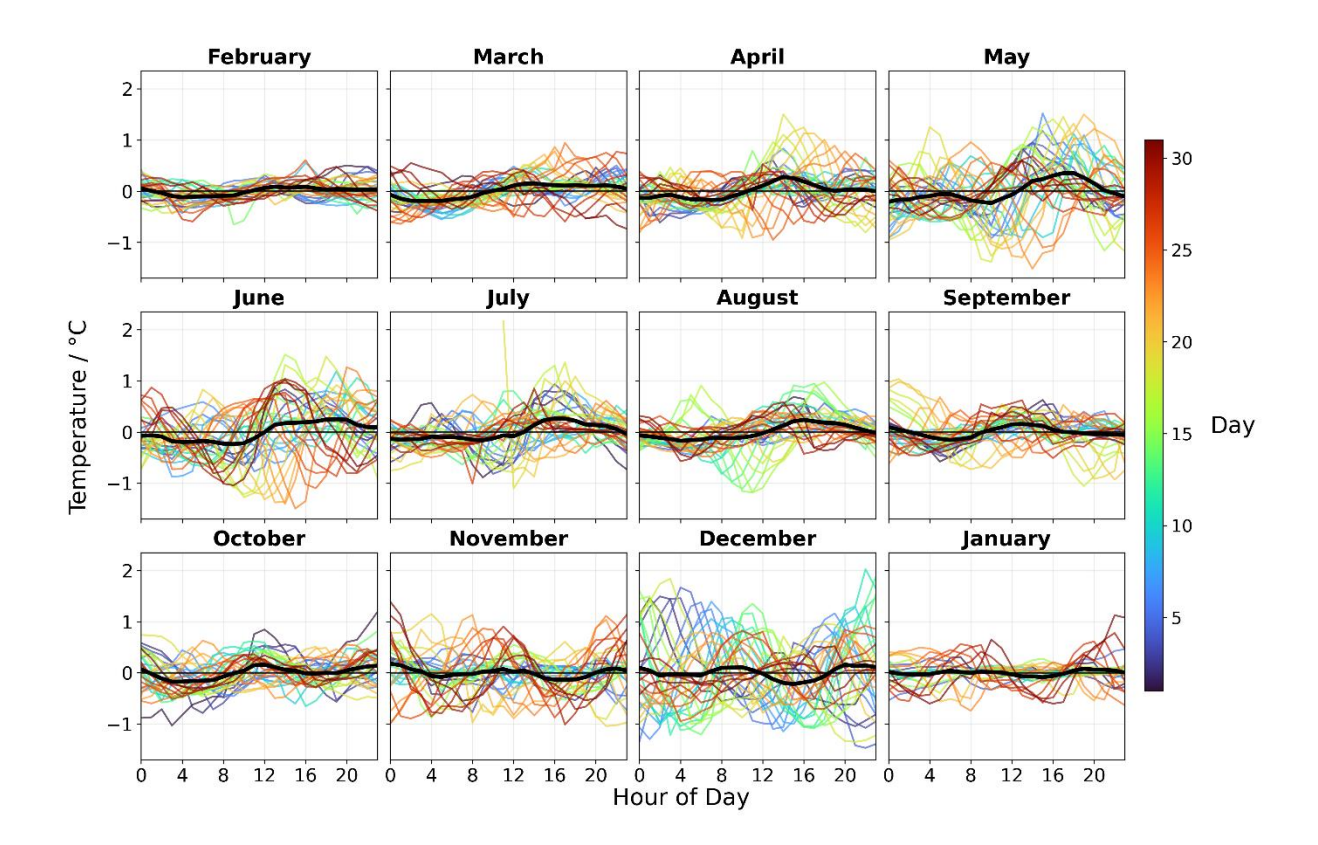


Figure S16. Seasonal diurnal variability of temperature anomalies between February 2022-January 2023.

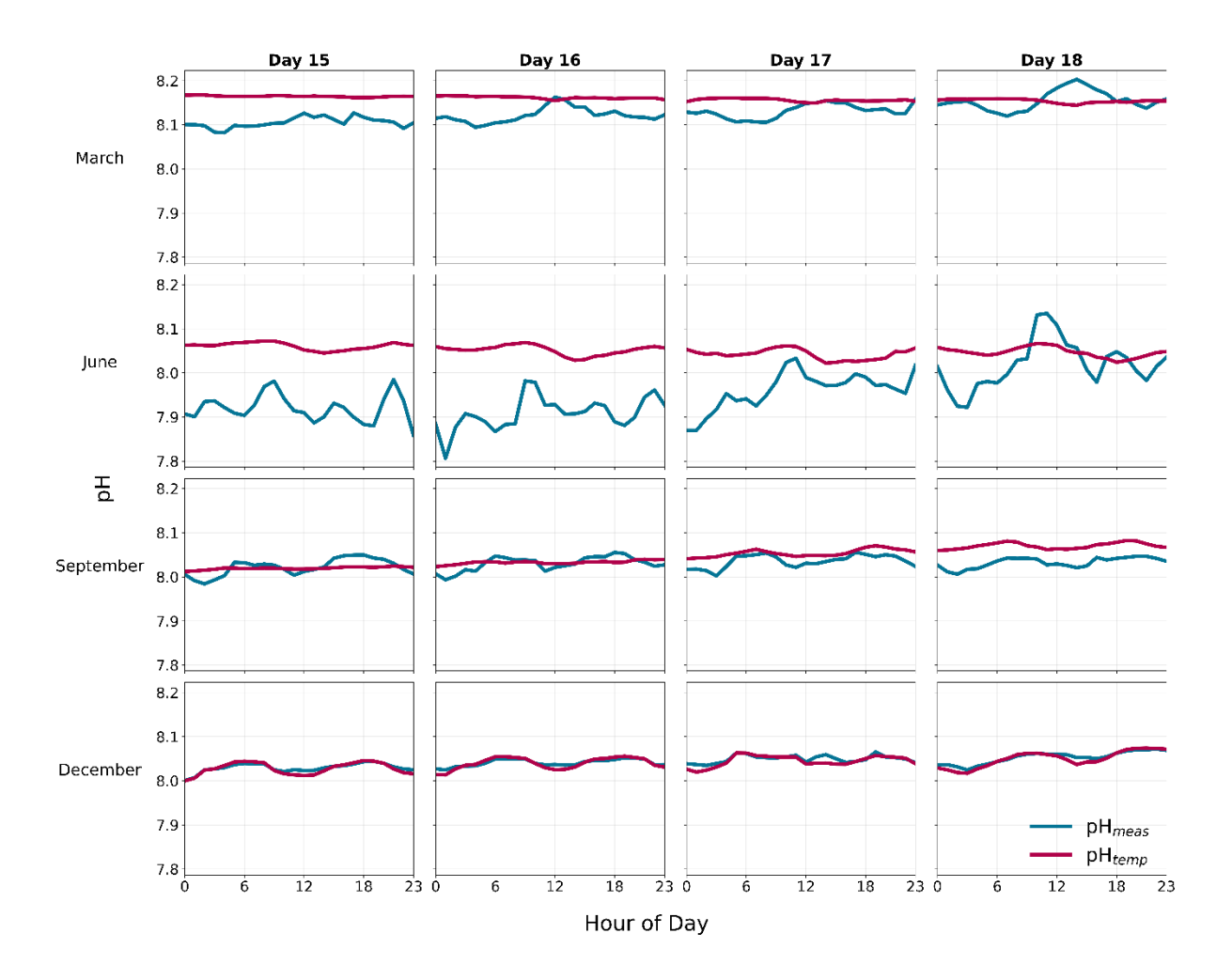


Figure S17. Comparison of pH_{meas} (blue) and pH_{temp} (red) across seasonal representative days in 2022. Four days (15-18) were selected from each month (March, June, September, December) to represent different seasonal conditions. Each subplot shows hourly mean pH values for each day.

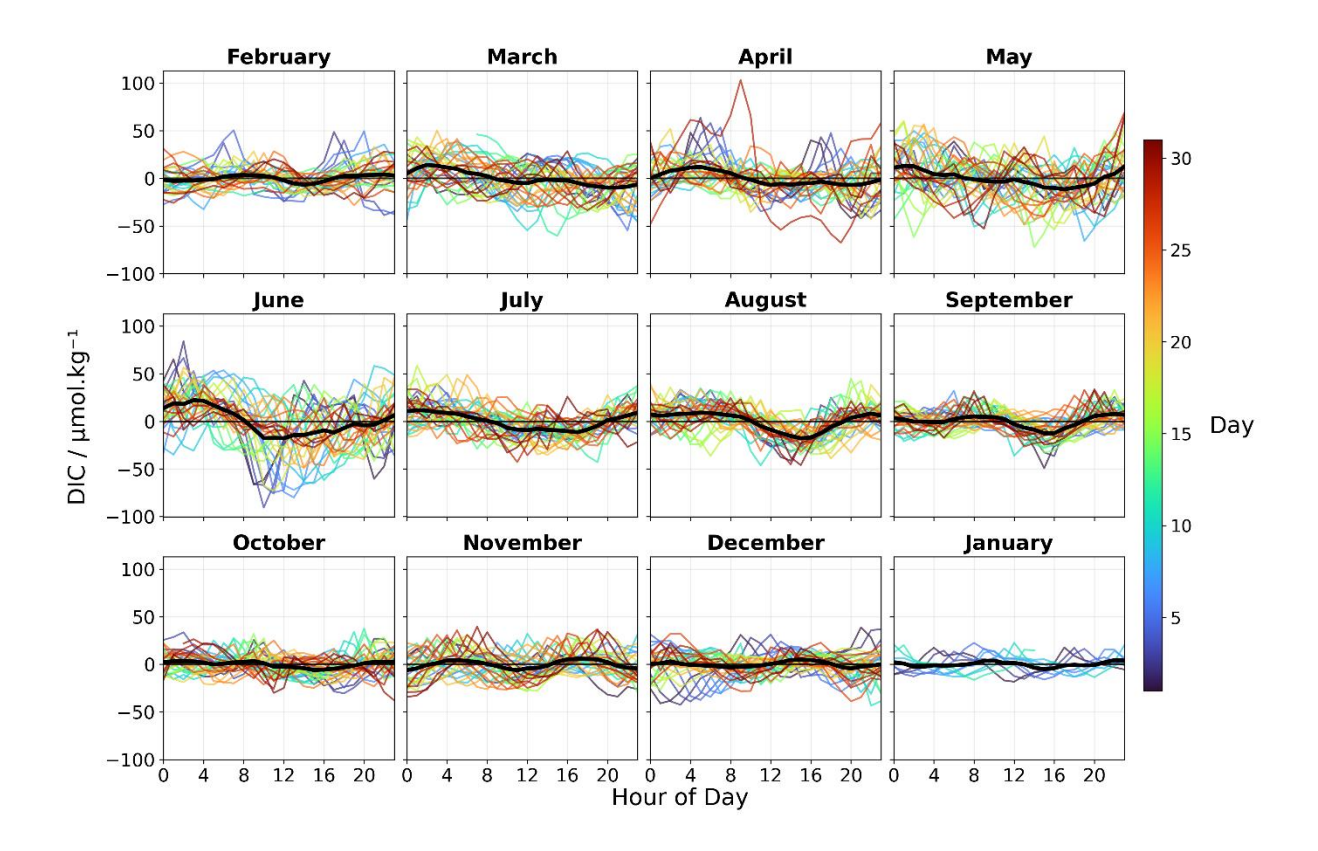


Figure S18. Seasonal diurnal variability of DIC anomalies between February 2022-January 2023.

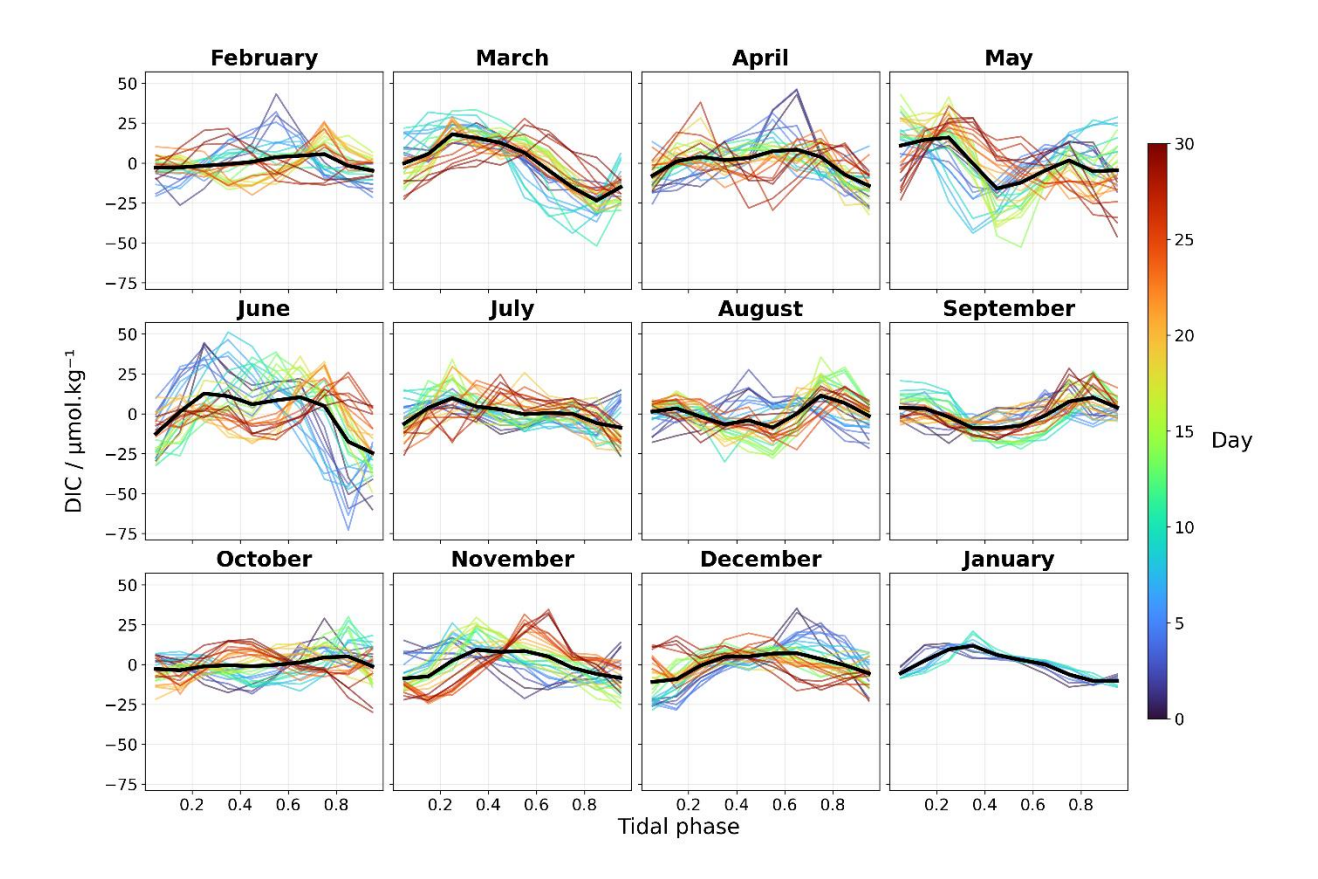


Figure S19. Tidal phase analysis variability of DIC anomalies between February 2022-January 2023.

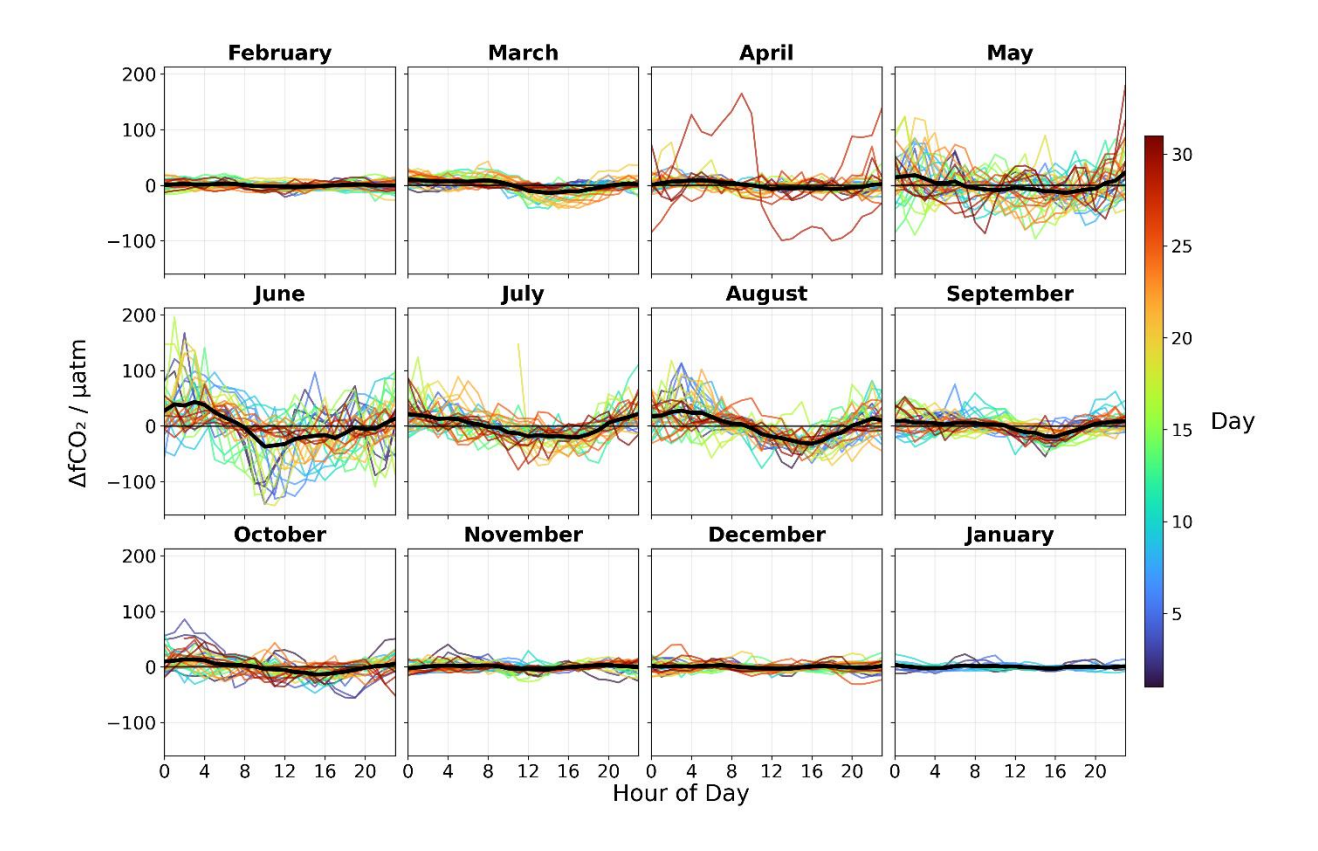


Figure S20. Seasonal diurnal variability of ΔfCO₂ anomalies between February 2022-January 2023.

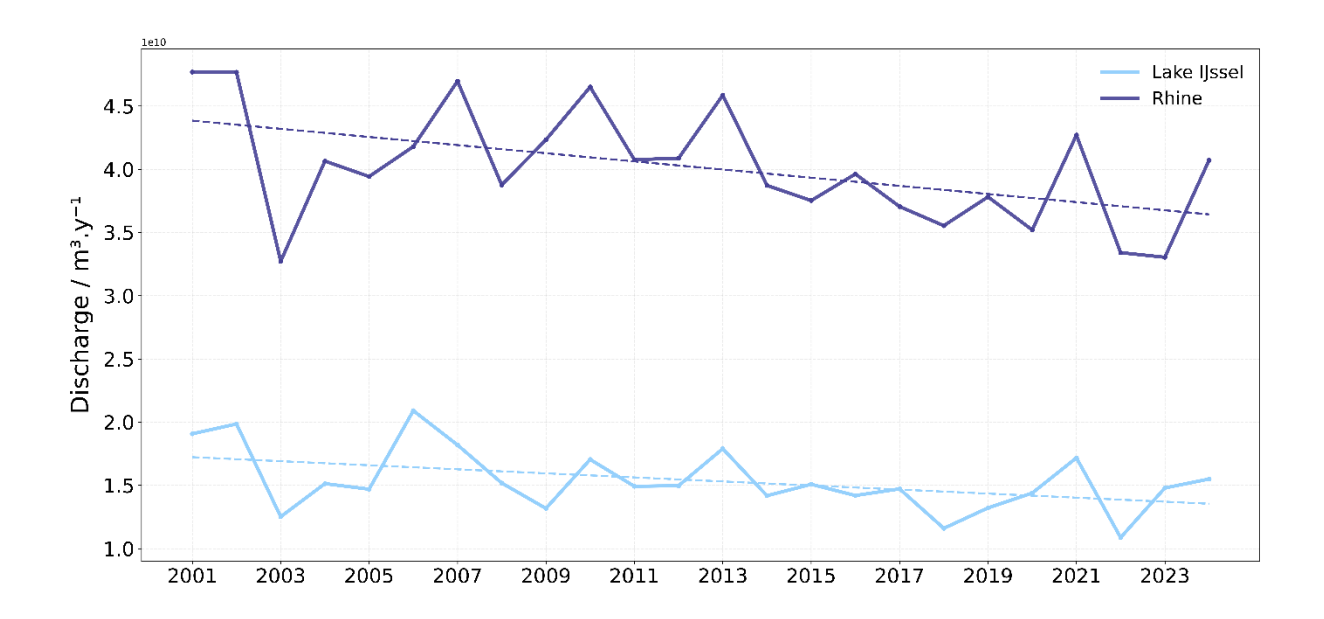


Figure S21. Yearly river discharge of the Rhine River (dark blue) and Lake IJssel (light blue) for the period 2001-2024. Discharge values are given in cubic meters per year (m³ y⁻¹).